4. Methods of characterization

4.1. X-ray Photoelectron Spectroscopy (XPS)

4.1.1. Basics of XPS

X-ray photoelectron spectroscopy was developed in the mid-1960's by Siegbahn and his research group at the University of Uppsala, Sweden [94]. It is based on the application of energy analysis of the electrons emitted from a surface illuminated by X-rays and exhibiting the photoelectric effect. It can be used to obtain information about the chemical composition and the chemical species present on the surface of plasma deposited films.

The sample is irradiated with X-rays of energy hν, which interact with the electrons in the sample via the photoelectric effect. Photoelectrons are emitted with a specific kinetic energy E_{kin} which is measured by an electron energy analyzer. This kinetic energy is given by,

$$E_{kin}=h\nu-BE-\phi_s \qquad \textbf{(Equation 4.1)}$$

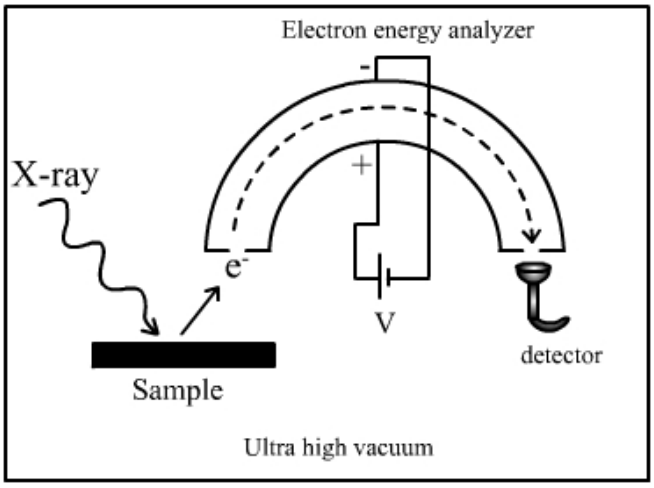

Figure 4.1: Schematic representation of working principle of XPS.

where BE is the binding energy of the atomic orbital from which the electron originates and ϕ_s is the spectrometer work function. The schematic representation of the working principle of an XPS instrument is shown in Figure 4.1. The spectrum is obtained as a plot of the number of detected electrons per energy interval versus their kinetic energy. Since the mean free path of the electrons in solids is very small, a majority of the detected electrons originate from the top few atomic layers. For electrons in the energy range 100 to 1000 electron volts (eV), the distance they travel without undergoing an inelastic collision,

known as the inelastic mean free path, may be typically of the order of 2 to 3 nm for the C1s, O1s and N1s core levels of organics. This distance corresponds to perhaps 10 atomic layers in most materials, and it is this that gives the technique its surface sensitivity. The electron mean free path as a function of electron kinetic energy follows a "universal curve" shown in Figure 4.2 [95] where the shaded region indicates the variations found in different materials. Experimentally, this inelastic mean free path is very difficult to measure and in practice, a parameter known as the attenuation length, which also includes the effect of elastic scattering, is determined instead.

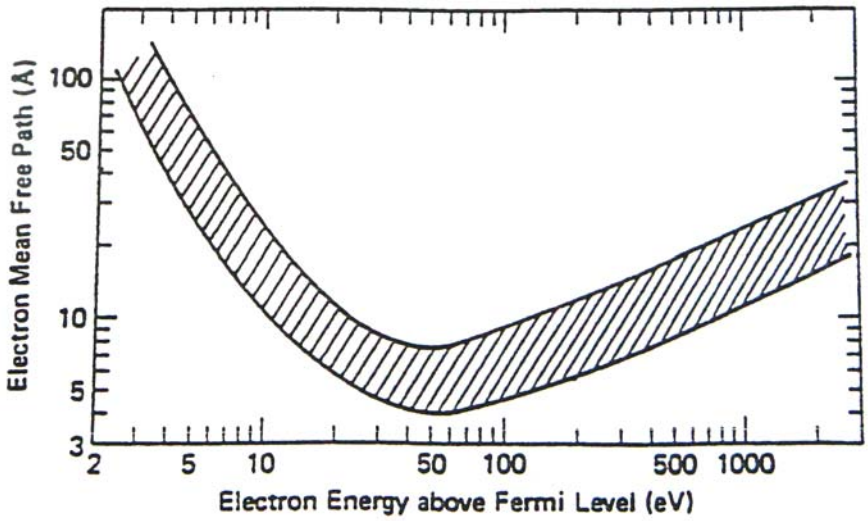

Figure 4.2: Electron mean free path as a function of electron kinetic energy above the Fermi level. The shaded area represent the distribution typically found for different materials.

Since the core levels of each element have unique binding energies, XPS can be used to identify and determine the concentration of the elements in the surface. Variation in the elemental binding energies (chemical shifts), arising from differences in the chemical potential (Madelung potential) and polarizability of compounds can be used to identify chemical states of the elements in materials being analyzed.

Two relaxation processes, the Auger decay and the fluorescent decay follow the photoionization process (Figure 4.3). In an Auger process, a transition of an outer electron to the inner orbital vacancy occurs, and another electron is simultaneously emitted, carrying off the excess energy, while in the fluorescent decay the excess energy is emitted in the form of X-ray fluorescence photons. For K shell ionizations, the probability of Auger decay is favored to that of a fluorescent decay.

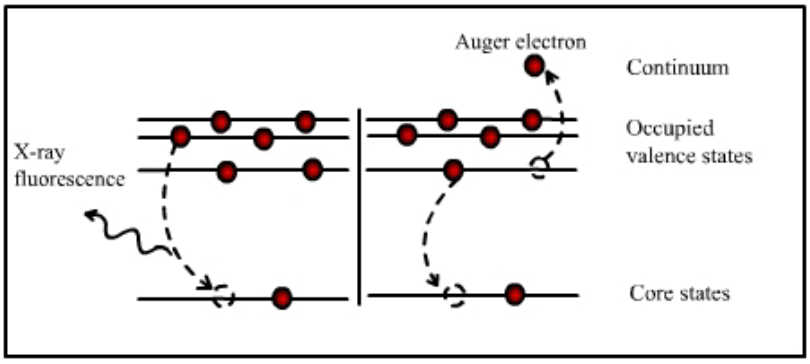

Figure 4.3: Schematic representation of the two core level relaxation processes.

Although an XPS spectrum contains Auger peaks along with photoelectron peaks the most intense peaks are typically the photoelectron peaks. The peak width of these peaks is a convolution of (a) the natural line width which is determined by the lifetime of the hole resulting from the photoionization process, (b) the width of the exciting X-ray line (c) the instrumental contribution to the observed line width and also (d) due to the solid state effects. One of the most valuable properties of core level photoelectron spectroscopy is the "Chemical shift". It implies that the detailed core level binding energy for an atom of a certain element depends on the first coordination sphere of the probed atom. If we consider a core level, the energy of an electron in this core state is determined by the Coulomb interaction with the other electrons and the attractive potential of the nuclei. Any change in the chemical environment of the element will involve a spatial redistribution of the valence electron charges of this atom and the creation of a different potential as seen by a core electron. This redistribution affects the potential of the core electrons and results in a change in their binding energies. Figure 4.4 shows an example of chemical shift related to this work. It shows the C1s spectrum of a plasma deposited allyl alcohol sample. The C1s binding energy of C-OR is shifted to higher binding energy by 1.5 eV if compared to the binding energy of pure hydrocarbon bonds such as CH_X. This is explained by the higher electronegativity of the oxygen atoms. If the electron density at the carbon atom is reduced, it results in a more positive effective charge at the nucleus and thus a higher binding energy of the electronic levels. Other chemical species such as C=O and COOR exhibiting different chemical shifts can also be observed in the Figure 4.4. Core levels show the chemical shifts, since they are localized at the atomic core and thus are sensitive to changes of the effective nuclear charge.

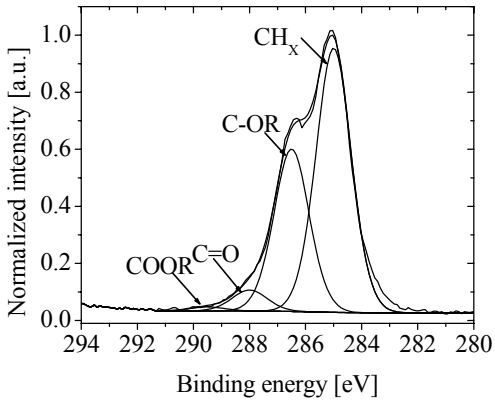

Figure 4.4: XPS C1s spectrum of a plasma deposited allyl alcohol sample showing the chemical shift for various species.

The removal of a core electron is also accompanied by substantial reorganization (relaxation) of the valence electrons in response to the effective increase in nuclear charge. This perturbation gives rise to a finite probability for photoionization to be accompanied by a simultaneous excitation of a valence electron from an occupied to an unoccupied molecular orbital (shake-up) or ionization by release of a valence electron (shake-off). These excitations reduce the kinetic energy of the emitted electrons and lead to satellite lines at higher binding energies in the photoemission spectra. The $\pi \rightarrow \pi^*$ shake-up features have been extensively used in this work to extract valuable information about the unsaturated or aromatic character of the plasma deposited films.

Peak intensities: To describe the peak intensities in the photoelectron spectra the photoelectric cross section σ has to be calculated. σ is defined as the probability P_{if} per unit time for the transition of electrons of an atom/molecule or solid from an initial state $|\Psi_i\rangle$ to a final state $|\Psi_f\rangle$ under the influence of electromagnetic radiation [95]. The transition probability P_{if} is given by Fermi's Golden Rule:

$$P_{if} \sim |\langle \Psi_f | H' | \Psi_i \rangle|^2 \, \delta(E_f - E_i - h\nu) = |M_{if}|^2 \cdot \delta(E_f - E_i - h\nu) \qquad \textbf{(Equation 4.2)}$$

with the transition matrix elements M_{if}

$$M_{if} = \langle \Psi_f | H' | \Psi_i \rangle \qquad \textbf{(Equation 4.3)}$$

The perturbation operator H' represents the electromagnetic radiation and can be approximated as

$$H' = \frac{e}{2mc}\left(\hat{p}.\hat{A} + \hat{A}.\hat{p}\right) \qquad \textbf{(Equation 4.4)}$$

where $\hat{p}$ is the momentum operator $-i\hbar\vec{\nabla}$ and $\hat{A}(\vec{r},\vec{t})$ is the vector potential of the electromagnetic field. The factor $\delta(E_f - E_i - h\nu)$ considers the energy conservation where E_f and E_i are the total energies in the final and initial state, respectively. $\hat{A}(\vec{r},\vec{t})$ can be written as

$$\hat{A}(\vec{r},\vec{t}) = \vec{e}.A_o.e^{i(\vec{k}.\vec{r}-\omega t)} \qquad \textbf{(Equation 4.5)}$$

where $\vec{e}$ describes the polarization direction of the radiation. In vacuum the Coulomb calibration can be applied ($\vec{\nabla}.\hat{A} = 0 \rightarrow \hat{p}.\hat{A} = 0$) and H' can be simplified to $2.(\hat{A}.\hat{p})$. If further the dipole approximation is applied, i.e. the term $e^{i\vec{k}.\vec{r}}$ is written as a series expansion and only the first term is taken into account, M_{if} can be written as

$$M_{if} \sim \langle \Psi_f | \vec{e}.\hat{p} | \Psi_i \rangle \qquad \textbf{(Equation 4.6)}$$

which is usually referred to as the dipole matrix element (DME). The dipole approximation is valid for $\vec{k}.\vec{r} << 1$.

The wave functions can be separated for the initial and final state of the electronic system according to:

$$\Psi_i = \hat{C} \,.\, \phi_{i,k}\, \Psi_i^R(n-1) \text{ and } \Psi_f = \hat{C} \,.\, \phi_{f,k}\, \Psi_{ljk}^{ion}(n-1), \qquad \textbf{(Equation 4.7)}$$

where $\phi_{i,k}$ and $\phi_{f,k}$ are the wave functions of the excited core electron in the initial and final state, respectively, Ψ_i^R and Ψ_{ljk}^{ion} are the wave functions of the not involved (n-1) electrons of the ground state and the ionic final state with a hole in the level k and a valence electron that was excited from a state j to the state l by the photoemission process. $\hat{C}$ is the antisymmetry operator for the wave functions. With these relations the transition matrix element M_{if} can be written as:

$$M_{if} = \langle \Psi_f | \vec{e}.\hat{p} | \Psi_i \rangle = \langle \phi_{f,k} | \vec{e}.\hat{p} | \phi_{i,k} \rangle \langle \Psi_{ljk}^{ion}(n-1) | \Psi_k^R(n-1) \rangle \quad \textbf{(Equation 4.8)}$$

In this case only the interaction of the electromagnetic radiation with the electron k is taken into account. This approximation considers the orbitals, that are not involved in the photoemission process as so-called "frozen orbitals", i.e. unchanged between initial and final state ($\Psi_{ljk}^{ion} = \Psi_k^R$). Now, the second factor in Equation 4.8 is equal to one and the transition matrix element is only the one electron matrix element. This approximation is called Koopmans's theory. In this case the core level spectrum of state k consists of only one symmetric peak at the binding energy known as Koopmans's energy. Of course, this approach does not take the intraatomic (extra atomic) core hole screening process into account. Thus, for a better description, the relaxed wave function Ψ_{ljk}^{ion} has to be considered and thus the different integrals are included, that described the intensity of the main peak and of its satellites. The intensity of each peak is then given by [96]:

$$I_{ij} \sim M_{ij}^2 \, \delta \, (E_{f,kin} + E_{lj}(n-1) - E_i(n) - h\nu) \quad \textbf{(Equation 4.9)}$$

where $E_{lj}(n-1)$ is the energy of the excitation $j \rightarrow l$ and E_i the initial energy in the ground state. The intensity of a particular core level is now split between the main peak [(l;j)=0] and its satellites [(l;j)≠0] (shake-up), including the excitation into the continuum (∞;j) (shake-off).

Charging: In XPS, the samples often become positively charged as a result of the loss of electrons in the photoemission process. However, the standard twin-anode X-ray source (such as used in this study) also generates a significant number of low energy electrons as a result of photoemission from the X-ray window. Some of these may be attracted to the positively charging sample, and may partially neutralize its charge. Despite this, the spectrum is always found to be shifted by a few electron volts from their expected energies. In such case, it is a common practice to identify the CH_X component, note its energy difference from the expected reference value, and apply the same shift to all other peaks in the spectrum before making any chemical state assignments. The common binding energy reference value used for this CH_X component peak is 285 eV [97].

Quantitative analysis: It is also possible to determine the relative concentrations of the various elemental constituents of a sample surface by XPS investigations. There are

methods for quantifying the XPS measurement utilizing peak area and sensitivity factors. For a sample that is homogenous in the analysis volume, the number of photoelectrons per second in a XP spectrum is given by [98]:

$$I = n.J.\sigma(E_{kin}).D(E_{kin}).T.L.A.\lambda(E_{kin}).\cos\theta \qquad \textbf{(Equation 4.10)}$$

where n is the number of atoms of the element per cm^3 of the sample,

J is the X-ray flux in photons/cm^2.sec,

$\sigma(E_{kin})$ is the photoelectric ionization cross-section for the atomic orbital of interest in cm^2,

$D(E_{kin})$ is the detection efficiency for each electron transmitted by the electron spectrometer,

T is the analyzer transmission,

L is the angular asymmetry of the intensity of the photoemission from each atom,

A is the area of the sample from which photoelectrons are detected,

$\lambda(E_{kin})$ is the inelastic mean free path of the photoelectrons in the sample,

θ is the angle of emission of the electrons measured from the surface normal.

Equation 4.10 leads to

$$n = I/J.\sigma\,(E_{kin}).D(E_{kin}).T.L.A.\lambda(E_{kin}).\cos\theta \qquad \textbf{(Equation 4.11)}$$

The denominator in the Equation 4.11 can be defined as the atomic sensitivity factor, S. If a peak from each of two elements is considered, then:

$$n_1/n_2=(I_1/S_1)/(I_2/S_2) \qquad \textbf{(Equation 4.12)}$$

This expression may be used for all homogenous samples. Thus, for any spectrometer, it is possible to develop a set of relative values of S for all of the elements. Multiple sets of values are necessary for instruments with multiple X-ray sources at different angles relative to the analyzer and different X-ray energies.

A general expression for determining the atomic fraction of any constituent in a sample, C_x, can be written as an extension of the Equation 4.12:

$$C_x = \frac{n_x}{\sum n_i} = \frac{I_x/S_x}{\sum I_i/S_i} \qquad \textbf{(Equation 4.13)}$$

4.1.2. Instrumentation of XPS

A VG Scientific ESCAlab 200X electron spectrometer was used to acquire the XP spectra. It consists of a double anode X-ray tube, a hemispherical energy analyzer and an

electron detector. The samples could be excited by Al Kα or Mg Kα radiation of which the photon energies are 1486.6 eV and 1253.6 eV, respectively. In this work Mg Kα radiation was employed with the gun operated at 15 kV and 20 mA, due to its lower FWHM. The electron analyzer acts as an energy filter, which allows passing electrons possessing a certain kinetic energy with a small half width. The spot size of the analyzer system was adjusted to a diameter of 3 mm. After passing through the analyzer, the electrons reach the detector where they are detected by channeltrons. For the spectral analysis and chemical interpretation the softwares CASA (Kratos) and Eclipse 2.0 (VG -Scientific, UK), were used. Survey scans used for quantification purpose were recorded in the CRR (Constant retard ratio) 10 mode because the spectrometer transmission function is known for this mode. Highly resolved spectra were recorded in the CAE (Constant analyzer energy) 10 mode. The vacuum in the spectrometer was in the range of 10^{-9} mbar during the measurements. A flood gun was not used for charge compensation. The spectrometer energy scale was calibrated following ISO 15472.

4.2. Near-edge X-ray absorption fine structure (NEXAFS)

4.2.1. Basics of NEXAFS

While direct photoemission spectroscopy offers an experimental approach to the occupied electronic states and bands of a solid, NEXAFS (Near-Edge X-ray Absorption Fine Structure) spectroscopy is a technique to characterize surfaces by evaluation of unoccupied electronic states of the molecular orbitals.

In NEXAFS spectroscopy the X-ray absorption is measured by scanning the photon energy hν across an absorption edge. If hν exceeds the ionization energy E_i of the investigated level, the electrons are emitted as photoelectrons, and a high absorption cross-section is detected. At $h\nu=E_i$ the well-known X-ray absorption edges are observed. However, besides these excitations into continuum states, additional very distinct resonant excitations of core level electrons into unoccupied molecular orbitals can also occur below the ionization energy (Figure 4.5). These final states such as the LUMO (lowest unoccupied molecular orbital), falling below the ionization potential correspond to bound states and the excited electrons do not leave the molecule. The respective spectral features are termed as π* resonances. These resonances have small lifetime widths leading to sharp distinct peaks below the ionization potential. On the other hand the final states above the ionization potential, where the excited photoelectrons are in quasi-bound electronic states

are termed as σ* resonances. The energy width of the σ* resonance is related to the lifetime of the quasi-bound electronic state. Because of the increasing decay probability of the electrons to continuum states, σ* resonances become broader the higher they lie in the continuum.

The LUMO as well as the HOMO (highest occupied molecular orbital) often have π character, which is particularly the case for the molecules investigated in this work. Note, that the unoccupied, non-bonding molecular orbitals are marked by asterisks (*).

As already discussed in the XPS case, the core holes relax via the emission of fluorescence X-rays or release of Auger electrons. The number of generated Auger electrons during the relaxation process is directly proportional to the respective X-ray absorption cross-section.

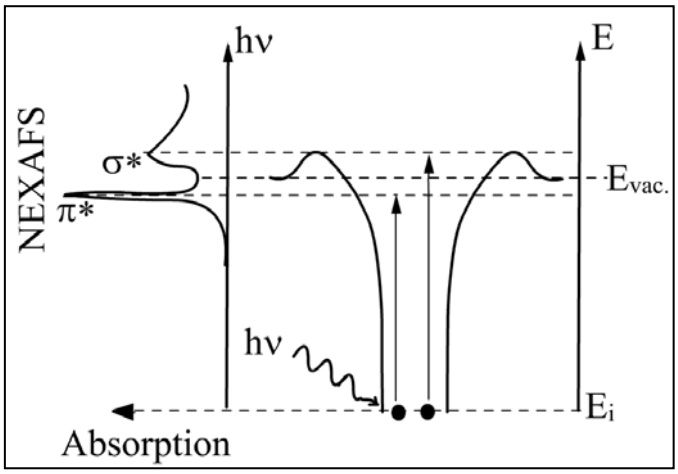

Figure 4.5: Schematic representation of an X-ray absorption process showing NEXAFS by the example of a diatomic molecule.

There are various modes of experimentation in the absorption spectroscopy experiments. One way to measure the absorption signal is to measure the transmitted photon flux with an X-ray detector behind the sample. However, this method is restricted to samples with optical densities below the total absorption limit, e.g. thin (<250 nm) polymer films.

The fluorescent decay of the core hole is used as the basis for the absorption measurement in the Fluorescent Yield (FY) experiments. In the case of Total Electron Yield (TEY) Auger and secondary electrons are detected, while in the case of Partial Electron Yield (PEY) electrons of kinetic energy larger than a particular threshold energy

are detected. While the FY technique is a bulk method TEY and PEY modes are used for surface sensitive measurements. Similar to XPS the surface sensitivities of TEY and PEY modes depend on the electron mean free path and can be derived from the Figure 4.2. In this work TEY mode was used without exception. The charging introduced in the sample by the loss of electrons makes this mode more surface sensitive.

4.2.2. Instrumentation of NEXAFS

The NEXAFS spectra of the samples were obtained in the total electron yield (TEY) mode. These were obtained with a high-energy spherical grating monochromator using 150 μm slits at the beamline station HESGM of the synchrotron radiation source BESSY II, Berlin. The resolution $E/\Delta E$ of the used grid I at the carbonyl resonance at $h\nu$ = 287.4 eV was found to be in the order of 2500.

Raw spectra were divided by the monochromator transmission function, which was obtained with a freshly sputtered Au sample. The spectra were recorded at an angle of 55^{o}, measured between the surface plane of the sample and the direction vector of the incident, linearly polarized light beam. Energy alignment of the energy scale was achieved by calibrating the characteristic features in the flux monitor signal (I_o) with a pyrolytic graphite sample (Advanced Ceramic Corp., Cleveland, USA) [99]. Spectra are shown with the pre-edge count rate subtracted and after normalization in units of the absorption edge jump [95].

4.3. Error estimates

The reported XPS values for O/C atomic ratio, component areas or FWHM of component peaks (after fitting of peaks) in this work have an estimated statistical error of 5-10%. These estimates where made in accordance with the theory discussed in reference [100]. The reported NEXAFS values have an estimated statistical error of <5%.